Factors affecting drying and wetting soil-water characteristic curves of sandy soils

Hong Yang, Harianto Rahardjo, Eng-Choon Leong, and D.G. Fredlund

Abstract: Drying and wetting soil-water characteristic curves (SWCCs) for five sandy soils are investigated using a Tempe pressure cell and capillary rise open tube. The test data are fitted to two SWCC equations using a least-squares algorithm. The obtained fitting parameters and some hysteretic behaviour are discussed and correlated with grain-size distribution parameters. A concept of total hysteresis is proposed to quantify the hysteresis of SWCC. The measured SWCC for one soil is also compared with the SWCC estimated from its grain-size distribution. The SWCC was also obtained at a high dry density for one of the soils. The results show that the shapes of the SWCCs are similar to the grain-size distributions of the soils and are affected by the dry density of the soil. A coarse-grained soil has a lower air-entry value, residual matric suction, and water-entry value and less total hysteresis than a fine-grained soil. The residual matric suction and water-entry value tend to approach the same value when the effective grain size D_{10} of the soil is small, in the range of 3–6 mm. SWCCs of uniform soils have steeper slopes and less total hysteresis than those of less uniform soils. Soils with a low dry density have a lower air-entry value and residual matric suction than soils with a high dry density. The SWCC predicted from grain-size distribution is found to be sufficiently accurate.

Key words: soil-water characteristic curve, water content, suction, hysteresis, grain size.

Résumé : On a étudié les courbes caractéristiques sol-eau de mouillage et de séchage (SWCCs) au moyen de la cellule de pression Tempe et d'un tube ouvert d'ascension capillaire. Les données des essais ont été lissées à deux équations SWCC avec un algorithme des moindres carrés. On discute les paramètres de lissage et des comportements en hystérèse qui ont été mis en corrélation avec les paramètres de distribution granulométrique. Un concept d'hystérèse totale a été proposé pour quantifier l'hystérèse de la courbe SWCC. La courbe SWCC mesurée pour un sol a été aussi comparée à la courbe SWCC estimée en partant de sa distribution granulométrique. La courbe SWCC a été aussi obtenue à une haute densité sèche pour un des sols. Les résultats montrent que les formes des courbes SWCC sont similaires aux distributions granulométriques des sols et sont affectées par la densité sèche du sol. Un sol à gros grains a des valeurs plus faibles de la pression d'entrée d'air, de la succion matricielle résiduelle, et de la valeur de pression d'entrée d'eau, et a moins d'hystérèse totale qu'un sol à grains fins. La succion matricielle résiduelle et la valeur d'entrée d'air tendent à s'approcher de la même valeur lorsque D_{10} du sol est petit, d'environ 3 mm à 6 mm. Les courbes SWCC de sols uniformes ont des pentes plus abruptes et moins d'hystérèse totale que les sols moins uniformes. Les sols avec une densité sèche faible ont une valeur d'entrée d'air et de succion matricielle résiduelle plus faibles que les sols ayant une haute densité sèche. On a trouvé que la courbe SWCC prédite par la distribution granulométrique est suffisamment précise.

Mots clés : courbe caractéristique sol-eau, teneur en eau, succion, hystérèse, granulométrie.

[Traduit par la Rédaction]

1. Introduction

Numerous research works have demonstrated that the relationship between the water content and matric suction of a soil (i.e., the soil-water characteristic curve, SWCC) is central to the behaviour of an unsaturated soil (e.g., Fredlund and Rahardjo 1993*b*; Barbour 1998). The SWCC can be related to other properties describing the behaviour of the soil, such as the unsaturated coefficient of permeability (Fredlund et al. 1994) and the shear strength (Vanapalli et al. 1996).

An SWCC relates the gravimetric water content, *w*, or volumetric water content, θ_w (defined as the volume of water in the soil divided by the total volume of the soil, V_w/V), to soil suction. The shape of the SWCC is a function of soil type. Typical drying and wetting SWCCs are illustrated in Fig. 1. The air-entry value, AEV or ψ_a, is defined as the matric suction at which air first enters the largest pores of the soil during a drying process (Brooks and Corey 1964, 1966). As matric suction is increased from zero to the AEV of the soil, the volumetric water content of the soil, θ_w, is nearly constant. Then the water content steadily decreases to the residual water content, θ_r, as matric suction increases beyond the AEV. The residual water content is the water content at re-

Received 5 September 2002. 15 March 2004. Published on the NRC Research Press Web site at http://cgj.nrc.ca on 6 October 2004.

H. Yang, H. Rahardjo,[1] and E.-C. Leong. School of Civil and Environmental Engineering, Nanyang Technological University, Block N1, #A-03, 50 Nanyang Avenue, Singapore 639798.
D.G. Fredlund. Department of Civil Engineering, University of Saskatchewan, SK S7N 5A9, Canada.

[1]Corresponding author (e-mail: chrahardjo@ntu.edu.sg).

 doi: 10.1139/T04-042

Fig. 1. Idealized soil-water characteristic curves (modified after Fredlund and Xing 1994).

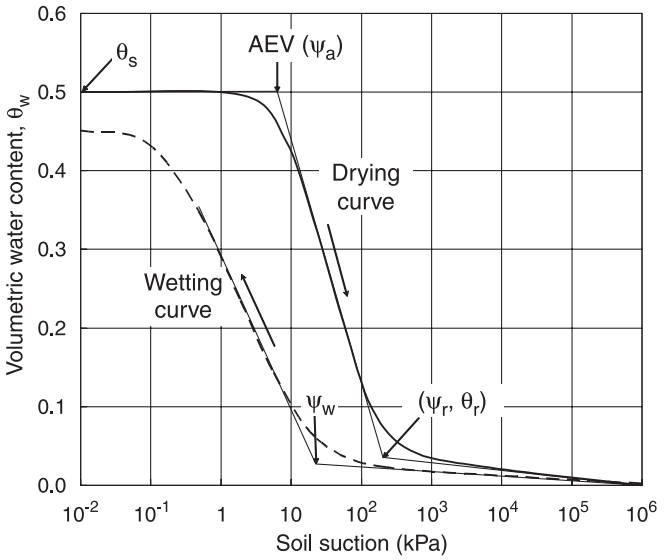

sidual state, at which water phase is discontinuous. The soil suction corresponding to the residual water content is called the residual soil suction, ψ_r. The water-entry value, ψ_w, on the wetting SWCC, is defined as the matric suction at which the water content of the soil starts to increase significantly during the wetting process.

A number of empirical models or equations have been developed to describe the highly nonlinear SWCC (e.g., van Genuchten 1980; Mualem 1986; Rossi and Nimmo 1994; Fredlund and Xing 1994; Assouline et al. 1998; Aubertin et al. 1998). Among these equations, the van Genuchten (1980) equation has been used by many researchers (e.g., Stormont and Anderson 1999). Leong and Rahardjo (1997) found the van Genuchten equation and the Fredlund and Xing (1994) equation to be the best SWCC models for a variety of soils. Therefore, the Fredlund and Xing and van Genuchten equations were used in this study. Both equations were used with a least-squares algorithm in the SoilVision computer software (SoilVision Systems Ltd. 1999) to fit the SWCC test data.

The Fredlund and Xing (1994) equation can be written as follows:

$$[1] \qquad \theta_w = \theta_s \left[1 - \frac{\ln(1+\psi/\psi_r)}{\ln(1+10^6/\psi_r)}\right]\left[\frac{1}{\{\ln[e+(\psi/a)^n]\}^m}\right]$$

where θ_w is the volumetric water content; θ_s is the saturated volumetric water content; a is a soil parameter related to the AEV of the soil, ψ_a (kPa); n is a soil parameter related to the slope at the inflection point (near the air-entry value) on the SWCC; m is a soil parameter related to the residual water content portion of the curve; e is the natural number 2.71828…; ψ is any soil suction (kPa); and ψ_r is the residual suction (kPa) corresponding to the residual water content, θ_r.

The van Genuchten (1980) equation can be written as follows:

$$[2] \qquad \theta_w = \theta_r - (\theta_s - \theta_r)[1 + (\psi/a_v)^{n_v}]^{m_v}$$

where θ_w, θ_s, θ_r, and ψ have the same meanings as in eq. [1]; a_v is a soil parameter related to the AEV; n_v is a soil parameter related to the rate of water extraction from the soil, once the AEV has been exceeded; and m_v is a soil parameter related to θ_r.

The fitting parameters in both eq. [1] (i.e., a, n, m, and ψ_r) and eq. [2] (i.e., a_v, n_v, and m_v) describe the shape of the SWCC. These parameters are obtained through best-fitting of test data to the computed SWCC using a least-squares algorithm. More details can be found in Fredlund and Xing (1994) and van Genuchten (1980). The fitting parameters, the values of ψ_a and ψ_r (and ψ_w for wetting SWCC), are determined using a computational construction technique with the aid of SoilVision computer software (SoilVision Systems Ltd. 1999), which involves establishing tangent lines to the SWCC (Fig. 1). The details of the technique are given in SoilVision Systems Ltd. (1999) and Vanapalli et al. (1998).

The SWCC of the soil can also be estimated from the grain-size distribution, and a number of methods for prediction have been developed (e.g., Gupta and Larson 1979; Arya and Paris 1981; Haverkamp and Parlange 1986; Fredlund et al. 1997; Aubertin et al. 2003). The method proposed by Fredlund et al. (1997) is based on the capillary model and knowledge of variation in the SWCC for various grain-size distributions of soils. The computation of the estimation based on the method of Fredlund et al. can also be performed using the SoilVision computer software (SoilVision Systems Ltd. 1999).

It is generally recognised that the volumetric water content of soil at a matric suction is not unique. For a given matric suction, water content in the drying curve is always higher than that in the wetting curve (Fig. 1). In other words, soil follows different SWCCs during a drying and a wetting process. This phenomenon is referred to as hysteresis. There have been a number of authors who have studied and proposed various models to predict the hysteretic behaviour of the SWCC, mainly to predict the wetting curves and the secondary curves, i.e., the curves between drying and wetting curves (e.g., Parlange 1976; Mualem 1977, 1984; Jaynes 1985; Hogarth et al. 1988; Nimmo 1992; Pham et al. 2003).

In this paper, the drying and wetting SWCCs for five sandy soils were tested and best-fitted using the Fredlund and Xing (1994) equation and the van Genuchten (1980) equation using SoilVision computer software (SoilVision Systems Ltd. 1999). The obtained fitting parameters and some hysteretic characteristics are discussed and correlated to grain-size distributions of the soils. The concept of total hysteresis is proposed to quantify the hysteretic behaviour of the SWCCs.

2. Materials and test methods

2.1. Material descriptions and basic properties

Five soils, namely gravelly sand, medium sand, fine sand, clayey sand I, and clayey sand II, were used in the study. Gravelly sand was crushed from fresh granite and was light grey to white. It was commercially obtained. Medium sand was a light brown construction sand obtained from a local construction site. Fine sand was a light grey beach sand collected from the local Changi Beach in Singapore. Clayey sand I was modified from the local sedimentary Jurong For-

Table 1. Basic properties of the soils.

	Gravelly sand	Medium sand	Fine sand	Clayey sand I	Clayey sand II
Unified Soil Classification System	SP	SP	SP	SC	SC
Specific gravity, G_s	2.62	2.60	2.65	2.64	2.59
Grain-size analysis results					
D_{60} (mm)	5.15	1.25	0.35	0.66	0.56
D_{30} (mm)	3.68	0.62	0.23	0.051	0.021
D_{10} (mm)	2.73	0.29	0.17	0.003	0.0005
Coefficient of uniformity, C_u	1.89	4.31	2.06	220	1120
Coefficient of curvature, C_c	0.96	1.06	0.89	1.31	1.58
Gravel content (larger than 4.75 mm; %)	49.9	0.8	0	0	0.2
Fines content (finer than 0.075 mm; %)	0	0.8	0.8	31.5	38.9
Atterberg limits (on minus 0.425 mm sieve fraction)					
Liquid limit, LL	—	—	—	31	48
Plastic limit, PL	—	—	—	21	27
Plasticity index, PI	—	—	—	10	21
Soil properties used in SWCC test					
Dry density of soil, ρ_d (Mg/m^3)	1.62	1.69	1.56	1.72	1.47
Void ratio, e	0.617	0.538	0.699	0.535	0.762
Porosity (%)	38.2	35.0	41.1	34.8	43.2

Note: D_{10} for clayey sand II is extrapolated from the grain-size distribution curve.

mation residual soil, and clayey sand II was an original Bukit Timah granitic residual soil taken from a construction site near the Singapore Island Country Club.

Basic soil properties were measured for the five soils. Specific gravity was measured for all soils using the American Society for Testing and Materials (ASTM) standard test method D854-92 (ASTM 1997*b*). Dry sieving analyses were performed on gravelly sand, medium sand, and fine sand using ASTM standard test method D422-63 (ASTM 1997*a*), and wet sieving analysis and hydrometer tests were performed on clayey sands I and II using ASTM standard test methods D1140-92 (ASTM 1997*c*) and D422-63 (ASTM 1997*a*), respectively. The grain-size distributions of the five soils are shown in Fig. 2. Atterberg limit tests were performed on clayey sands I and II using ASTM standard test method D4318-95 (ASTM 1997*f*). Based on their basic properties (Table 1), the soils were classified in accordance with the Unified Soil Classification System using ASTM standard test method D2487-93 (ASTM 1997*e*).

Fig. 2. Grain-size distributions of the soils.

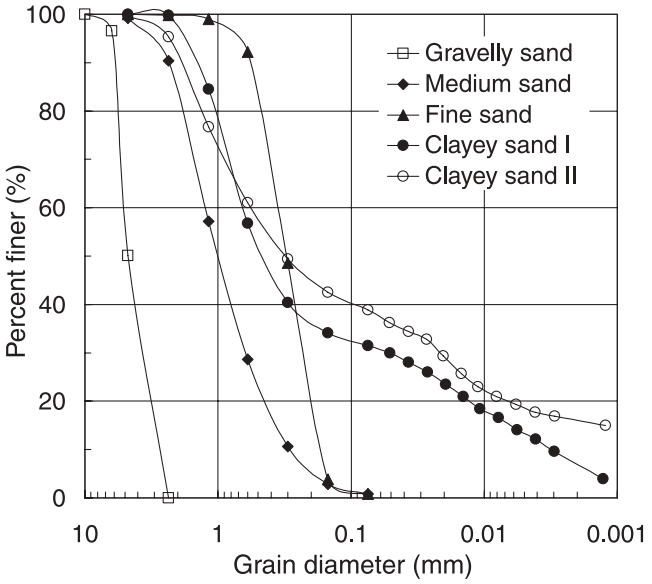

2.2. Drying soil-water characteristic curves using a Tempe pressure cell

Drying SWCCs for all the soils were determined using a Tempe pressure cell manufactured by Soilmoisture Equipment Corporation (1999). The Tempe pressure cell operates on the same principle as the conventional pressure plate apparatus described in ASTM D2325-68 (ASTM 1997*d*) (Fredlund and Rahardjo 1993*a*). A cross section of a Tempe pressure cell is shown in Fig. 3.

A dry soil specimen is first placed on a high-flow, high-air entry, ceramic disk inside the Tempe pressure cell. The high-flow, high-air entry ceramic disk in the Tempe pressure cell allows water to flow but stops the flow of air when it is saturated. An outlet is provided in the water compartment below the ceramic disk where water can drain from the soil specimen. Therefore, the water pressure is atmospheric (0 kPa) throughout the test and an air pressure is supplied through the inlet tube on the top cap. The top and bottom plates are fastened with bolts. O-ring seals keep the cell airtight during the test.

Before a Tempe pressure cell test was started, the soil was oven-dried and the mass of the soil required to achieve the target density was computed. The required amount of soil was placed in the Tempe pressure cell and compacted to the target density. The bolts on the Tempe pressure cell were tightened and the entire cell was submerged in water in a vacuum container and left for a few days for saturation. The Tempe pressure cell was then placed on a support ring that was placed in a tray filled with water (Fig. 4). Water level was maintained at the bottom of the soil specimen in the

Fig. 3. Cross section of a Tempe pressure cell (after Soilmoisture Equipment Corporation 1999).

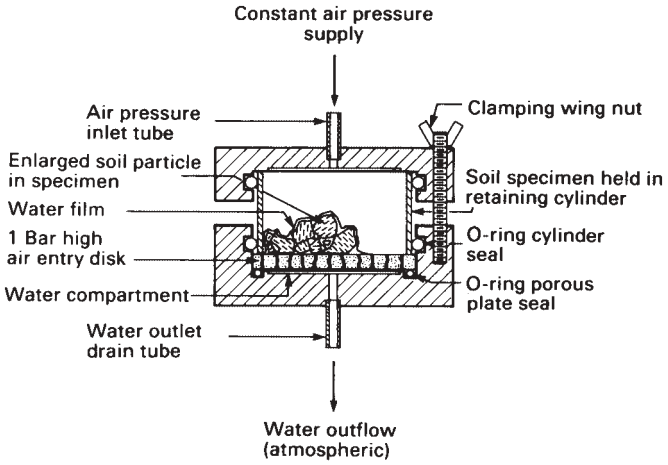

Fig. 4. Schematic diagram of setup of Tempe pressure cell test.

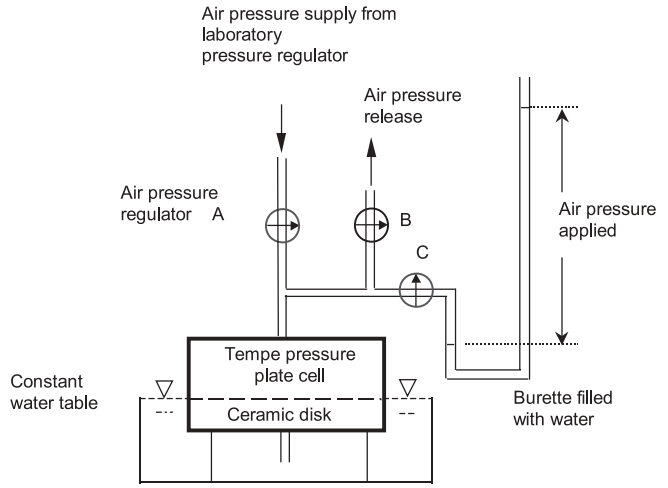

Tempe pressure cell. Before applying an air pressure, excess water at the surface of the Tempe pressure cell was removed. When the air pressure was set to the same value as the desired matric suction, water started to drain from the soil specimen through the ceramic disk until equilibrium was reached. The air pressure was not exactly equal to the matric suction, as discussed later in the paper. The change in water content of the soil specimen was measured by periodically weighing the entire Tempe cell. The weight of the Tempe pressure cell with respect to the elapsed time was plotted during the progress of the test to confirm equilibrium conditions. The procedure was then repeated at higher applied air pressures. After the application of the highest air pressure, the soil specimen was removed and the final water content was measured by oven-drying the soil specimen. The water contents corresponding to other applied matric suction values were found by back-calculation using the final water content and the previous changes in the weight of the Tempe pressure cell. The plot of water contents against corresponding matric suctions gave the SWCC.

As the air-entry values of some of the soils (e.g., gravelly sand and medium sand) used in the study were quite low, it

Fig. 5. Matric suction of a soil sample in Tempe pressure cell.

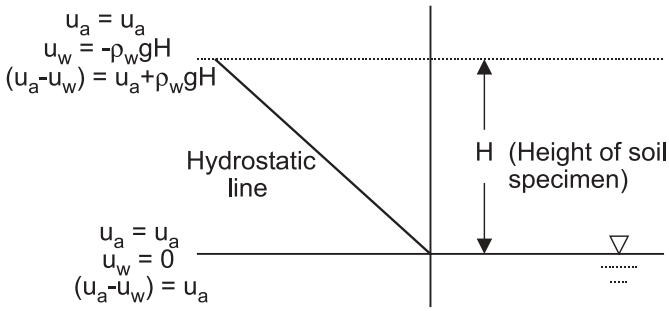

Fig. 6. Schematic diagram of capillary rise open tube.

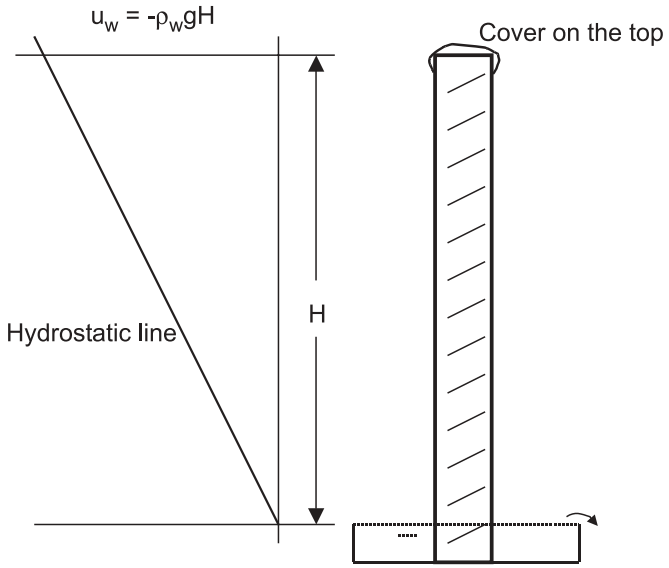

was desirable to start the test with a small matric suction in the order of 0.1 kPa (i.e., equal to 10 mm water head). The air pressure supplied through the existing pressure regulators in the laboratory was only accurate to 10 kPa. Therefore, two other air-pressure regulators (A and B in Fig. 4) were used to obtain air pressures that were lower than 10 kPa. The pressures were verified using a water head in a burette (Fig. 4). By adjusting regulators A and B, an air pressure as low as 0.1 kPa was obtained and sustained during the Tempe pressure cell tests.

When an air pressure, u_a (kPa), is applied to the Tempe pressure cell and equilibrium is reached, the matric suction is the average value of the matric suction in the soil rather than the value of the applied air pressure, u_a (kPa). This assumption is based on the negative hydrostatic pore-water pressure profile that is developed above the water table (i.e., bottom of the soil) at equilibrium (Fig. 5). The matric suction at the top and bottom of the soil is equal to $(u_a + \rho_w gH)$ and u_a, respectively. The actual matric suction can be calculated by taking the average value:

$$[3] \quad \text{average matric suction} = u_a + 0.5\rho_w gH$$

where ρ_w is the density of water (1.0 Mg/m^3); g is gravitational acceleration (9.81 m/s^2); and H is the height of the soil specimen (m).

Table 2. Results of the soil-water characteristic curves, the Fredlund and Xing (1994) and van Genuchten (1980) best-fit parameters.

Description	Symbol	Gravelly sand	Medium sand	Fine sand	Clayey sand I	Clayey sand II
Drying curve						
Saturated volumetric water content	θ_s	0.382	0.350	0.411	0.348	0.432
Air-entry value (kPa)	ψ_a	0.110	0.850	1.40	1.80	4.05
Residual matric suction (kPa)	ψ_r	0.401	3.75	3.94	11.4	14.9
Residual volumetric water content	θ_r	0.021	0.063	0.035	0.237	0.296
Fredlund and Xing best-fit parameters	a (kPa)	0.176	1.24	1.94	2.01	5.75
	n	4.44	4.39	6.30	3.92	8.98
	m	1.13	0.661	0.868	0.146	0.122
van Genuchten best-fit parameters	a_v (kPa)	0.139	0.940	1.67	1.34	3.47
	n_v	7.38	6.55	6.94	9.43	24.5
	m_v	0.198	0.129	0.238	0.0232	0.0128
Wetting curve						
Water-entry value (kPa)	ψ_w	0.285	3.18	2.69	19.1	506
Volumetric water content at ψ_w	θ_w	0.0074	0.0205	6.07×10^{-5}	0.108	0.106
Fredlund and Xing best-fit parameters	a (kPa)	0.07123	0.677	1.81	0.439	6.55
	n	1.23	1.62	3.19	1.29	0.497
	m	2.71	1.67	3.74	0.49	1.36
Van Genuchten best-fit parameters	a_v (kPa)	0.0481	0.629	1.95	0.345	8.81
	n_v	1.76	1.71	2.99	1.51	0.510
	m_v	0.669	0.643	1.79	0.176	0.684

Note: a and a_v are in kPa.

Fig. 7. Soil-water characteristic curves for gravelly sand (GS).

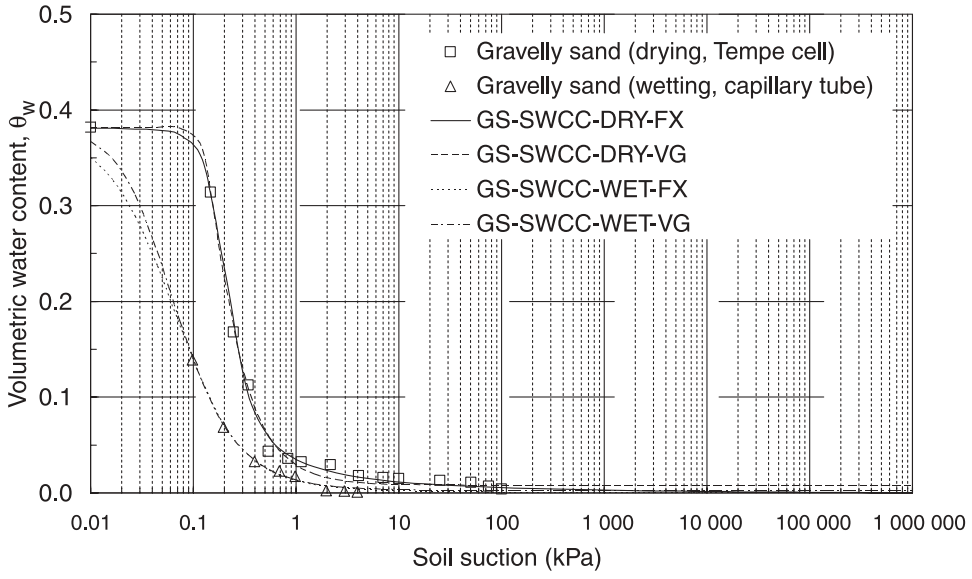

Equation [3] shows that a correction value of $0.5\rho_w gH$ (kPa) needs to be applied to obtain the actual matric suction. The shorter the soil specimen or the ring of the Tempe pressure cell, the smaller the correction will be. For a Tempe pressure cell with a 30 mm high ring as used in the study, the correction value is 0.15 kPa. This suggests that even under a zero air pressure ($u_a = 0$), the average matric suction in the soil is 0.15 kPa. This value may be negligible when the matric suction is high (e.g., a few hundred kPa), but it becomes significant for low matric suctions, particularly for coarse-grained soils where the air-entry value may be less than 1 kPa.

The volumetric water content, θ_w (volume of water divided by volume of soil), can be obtained from the gravimetric water content using the following equation:

$$[4] \qquad \theta_w = (\rho_d/\rho_w)w$$

Fig. 8. Soil-water characteristic curves for medium sand (MS).

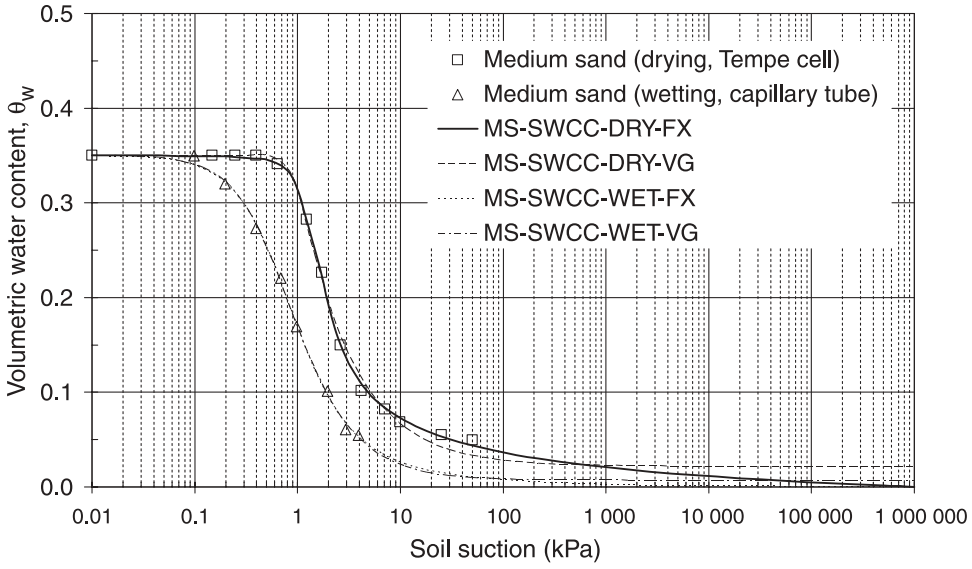

Fig. 9. Soil-water characteristic curves for fine sand (FS).

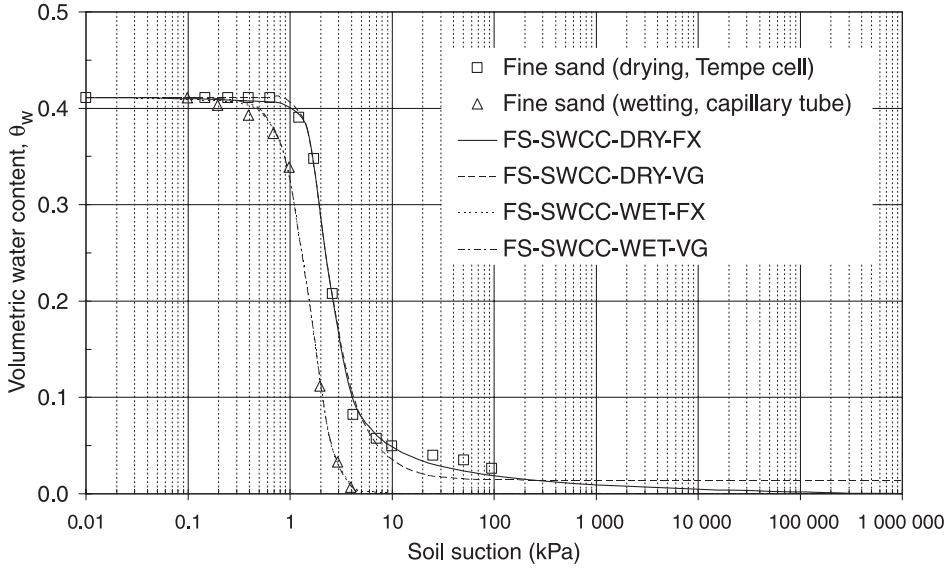

where w is the gravimetric water content (mass of water divided by mass of soil solids); ρ_d is the dry density of soil, which is known for the tests; and ρ_w is the density of water (1.0 Mg/m^3). The value of w at the end of a Tempe pressure cell test can be obtained by oven-drying the soil.

It is normally time-consuming to measure the SWCC. The required time depends on factors such as type of soil, size of soil specimen, applied air pressure, and type of ceramic disk (Topp et al. 1993). The equilibrium time for each applied suction varies from a few hours to a few days. ASTM standard test method D2325-68 (ASTM 1997*d*) suggests an equilibrium time of 18–48 h; Soilmoisture Equipment Corporation (1985) suggests 18–20 h; and Klute (1986) suggests an equilibrium time of 2–3 days, regardless of soil texture, matric suction, and whether the soil was drying or wetting. The tests in this study suggest that equilibrium conditions in a Tempe pressure cell test on sandy soils were generally achieved within 24 h at any applied suction level.

The soil specimen was initially saturated, and therefore the Tempe pressure cell test yielded a drying SWCC. Attempts were made to use the Tempe pressure cell to obtain the wetting SWCC by decreasing the air pressure from 100 kPa. Water was expected to flow back into the Tempe pressure cell, but this did not occur because the ceramic disk offers too great a resistance for the water to flow into the soil sample. The trial tests suggested that Tempe cells were not suitable for obtaining the wetting SWCC on coarse-grained soils.

2.3. Wetting soil-water characteristic curves using a capillary rise open tube

The wetting SWCC can be obtained using a capillary rise open tube (e.g., Lambe and Whitman 1979; Fredlund and Rahardjo 1993*a*). In the capillary tube test, soil is compacted in an open tube at a target dry density and placed in a tray with a water table maintained at the bottom of the tube

Fig. 10. Soil-water characteristic curves for clayey sand I (CSI).

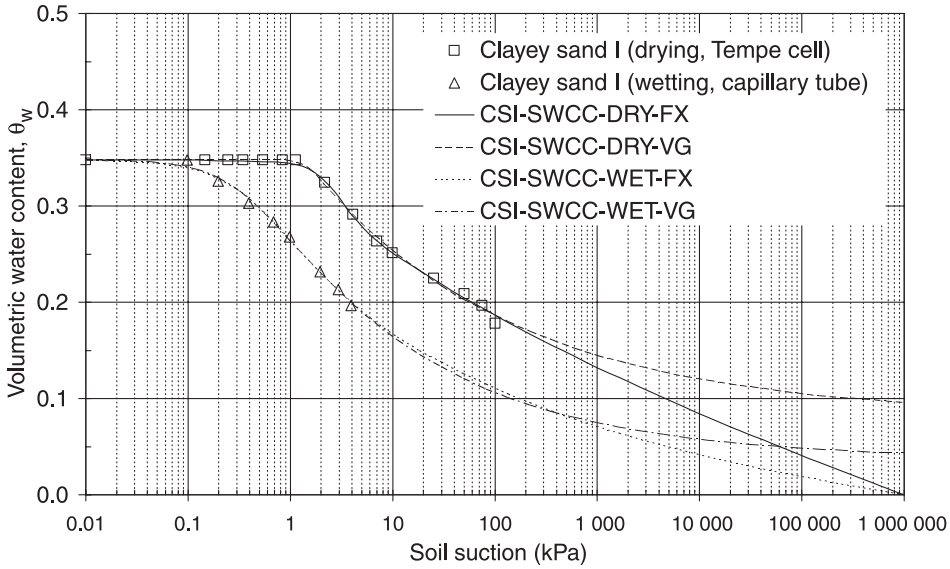

Fig. 11. Soil-water characteristic curves for clayey sand II (CSII).

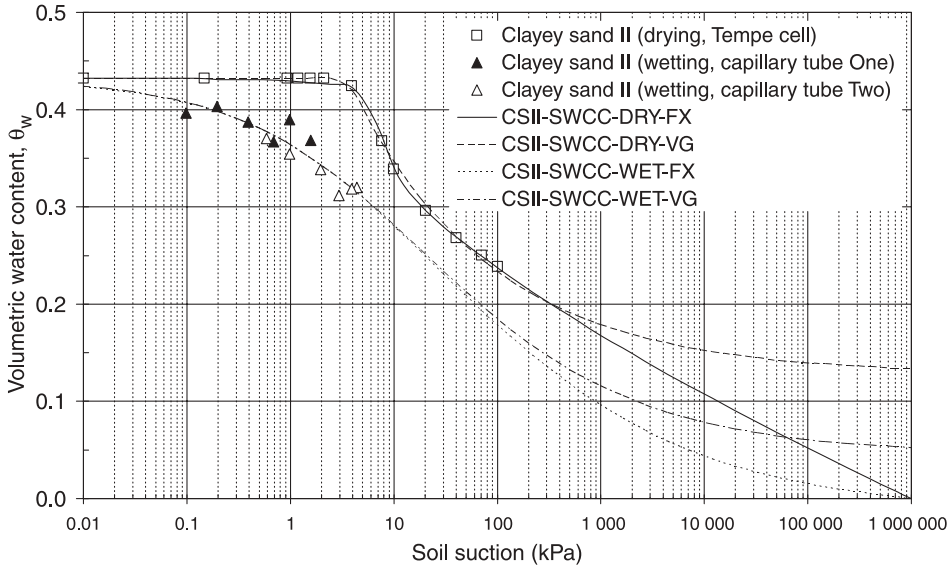

(Fig. 6). The top of the tube is covered to prevent evaporation. Water in the tray starts to move into the soil as soon as the tube is placed in the tray. After some time, equilibrium of the capillary water in the tube is reached. Soil samples can then be taken from various levels in the tube and oven-dried to determine the water content. The volumetric water content of the soil can be computed using eq. [4]. The height of a soil specimen above the water table is assumed to be equal to the capillary head (or negative pore-water pressure head) at that point. The magnitude of the negative pore-water pressure head is equal to the matric suction head, as the air pressure in the tube is atmospheric ($u_a = 0$). The plot of volumetric water content versus matric suction gives the wetting SWCC of the soil.

In this study, tubes 100 mm in diameter and 500 mm in length were used. Capillary tubes of soil were allowed to wet for 64 days. This period was considered sufficient for the soil tubes to reach equilibrium.

3. Results and discussion

3.1. Results of the soil-water characteristic curves

Drying soil-water characteristic curves (SWCCs) were obtained for the five soils using a Tempe pressure cell, and wetting SWCCs were determined using a capillary tube. The test data were best-fit using the Fredlund and Xing (1994) equation (the results are denoted FX). As a comparison, the SWCC test data were also best-fit using the van Genuchten (1980) equation (the results are denoted VG). The air-entry value, residual water content, residual matric suction, and fitting parameters of the SWCCs were found using the SoilVision computer software (SoilVision Systems Ltd. 1999) as listed in Table 2.

The test data and the best-fit SWCC results of the soils are shown in Figs. 7–11. The drying and wetting SWCC results for the five soils are also compiled in Figs. 12 and 13, respectively. The results indicate that the best-fit SWCCs us-

Fig. 12. Best-fit drying soil-water characteristic curves for the soils.

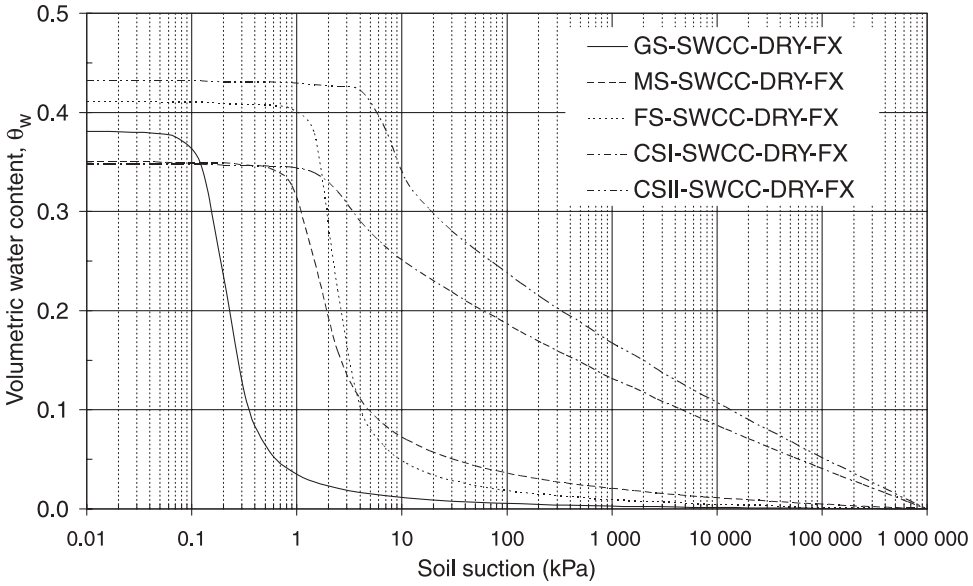

Fig. 13. Best-fit wetting soil-water characteristic curves for the soils.

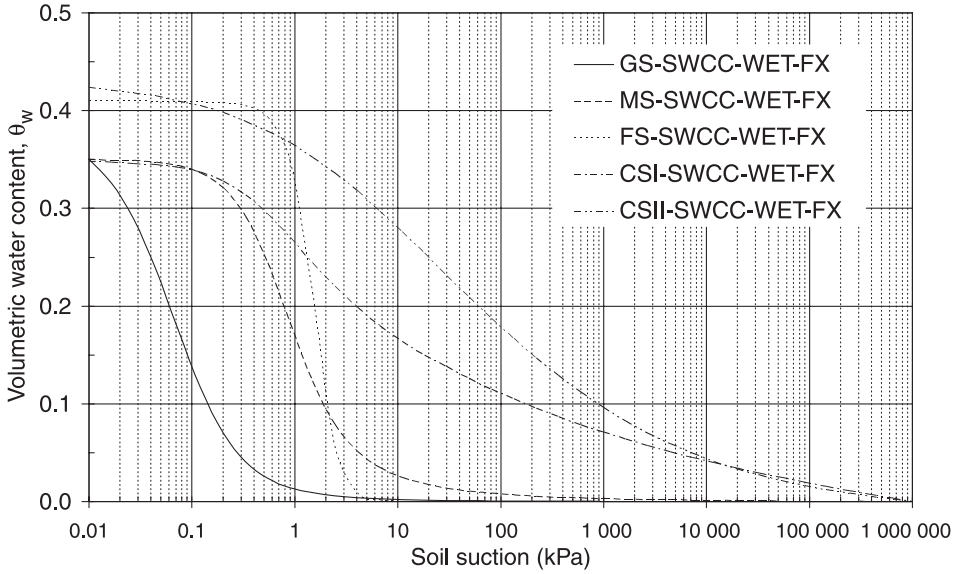

ing the Fredlund and Xing (1994) and van Genuchten (1980) equations closely describe the SWCC data of the soils and are sufficiently accurate to predict the SWCC up to the residual water content. Both equations are essentially the same for each of the five soils in the study, since both equations are of a similar generic form (Leong and Rahardjo 1997). The best-fit parameters of the Fredlund and Xing equation are discussed further in the study.

3.2. Relationship between drying soil-water characteristic curves and fitting parameters

The results show that the five soils have significantly different drying SWCCs (Fig. 12). The differences of the SWCCs are determined by the differences of the SWCC parameters, i.e., the air-entry value, ψ_a, residual soil suction, ψ_r, and best-fit soil parameters of a, n, and m. Gravelly sand has the smallest ψ_a of 0.11 kPa and the smallest ψ_r of 0.40 kPa among the five soils, and clayey sand II has the largest ψ_a of 4.05 kPa and the largest ψ_r of 14.9 kPa (Table 2). Corresponding to the relative magnitudes of the ψ_a of the soils, gravelly sand has the smallest a value of 0.176 kPa and clayey sand II has the largest a value of 5.75 kPa.

The SWCC parameters can be correlated to the fitting parameters. The ψ_a values of the soils and the soil parameter a are closely related and have an apparent linear relationship as shown in Fig. 14. The larger the ψ_a value, the greater the a value. The parameter a and the ψ_a value are not the same in both the Fredlund and Xing (1994) and van Genuchten (1980) equations (Leong and Rahardjo 1997), however. Similarly, the soil parameter m is related to the ψ_r value of the

Fig. 14. Soil parameter *a* in Fredlund and Xing (1994) equation versus air-entry value for the drying soil-water characteristic curves. R^2, correlation coefficient.

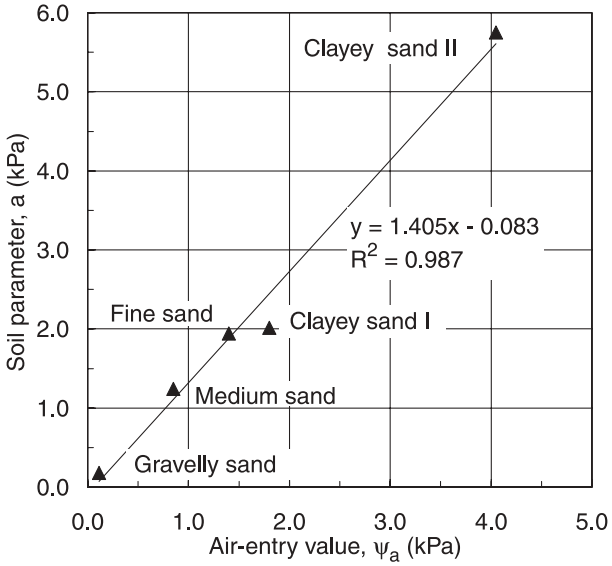

Fig. 15. Soil parameter *m* in Fredlund and Xing (1994) equation versus residual matric suction for the drying soil-water characteristic curves.

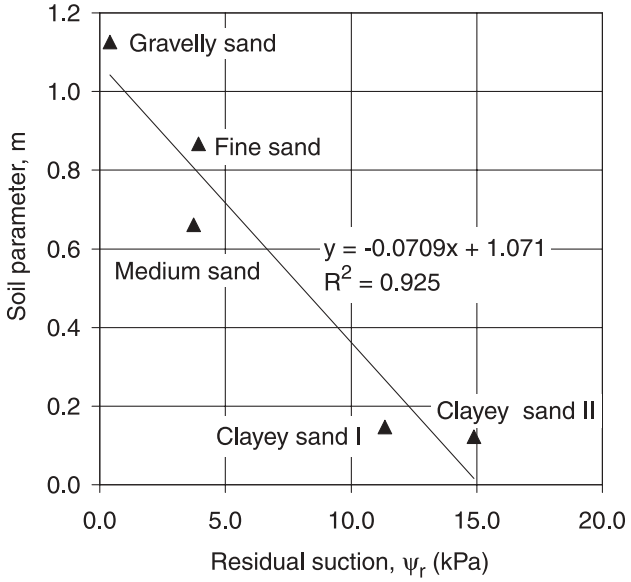

soil. The larger the ψ_r value, the smaller the *m* value (Fig. 15), which is also consistent with Leong and Rahardjo (1997). The slope of the SWCC for the portion between ψ_a and ψ_r is related to the parameter *n*. The slope of the SWCC can be measured as $[(\theta_s - \theta_r)/(\log\psi_r - \log\psi_a)]$. Generally, the steeper the slope of the SWCC, the larger the parameter *n* (Fig. 16). More discussions of the effect of soil parameters *a*, *n*, and *m* on the SWCC can be found in Fredlund and Xing and Leong and Rahardjo.

3.3. Relationship between drying soil-water characteristic curves and grain-size distribution and porosity

The SWCC is related to the pore-size distribution of the soil, which is in turn related to the grain-size distribution and porosity. Since it is common to assume that the average pore diameter is about 20% of the effective grain size, D_{10} (i.e., the grain diameter in mm corresponding to 10% passing by mass) (Holtz and Kovacs 1981), it is possible to relate D_{10} of a soil to its SWCC parameters of AEV and residual soil suction. The results show that both the AEV and residual soil suction of the drying SWCCs correlate well with the D_{10} of the soils (Fig. 17). A fine soil (i.e., a soil with small D_{10} or small pores) has a large AEV and a large residual soil suction.

The AEV and the residual soil suction of a soil decrease when the D_{10} of the soil increases. The difference between the AEV and the residual soil suction also decreases following a decrease of D_{10}. When the D_{10} of the soil decreases to a magnitude of 1–10 mm (or, more accurately, 3–6 mm), the AEV and the residual soil suction appear to approach the same value, that is, close to zero (Fig. 17). It is noted that the porosities of the soils in the study were comparable, although not exactly the same (Table 1).

The slope of the SWCC is also consistent with the slope of the grain-size distribution curve of the soil (Fig. 18). A steep slope on the grain-size distribution curve results in a

Fig. 16. Soil parameter *n* in Fredlund and Xing (1994) equation versus slope of the drying soil-water characteristic curves.

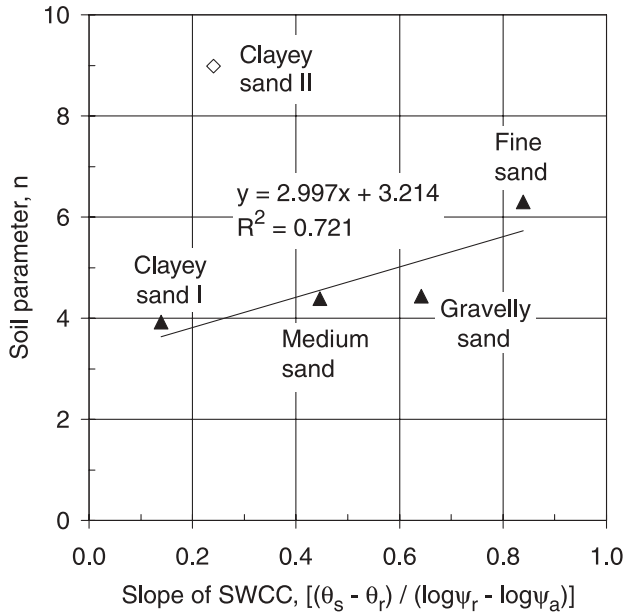

steep slope on the SWCC. This observation indicates that the drying SWCC of the soil is closely related to the grain-size distribution of the soil. Therefore, many empirical methods were developed to directly predict the SWCC from the grain-size distribution of the soil. One of the methods was proposed by Fredlund et al. (1997). As an example, the estimated SWCC for fine sand is shown in Fig. 19, which shows close agreement with the test data of the drying SWCC. These observations suggest that the drying SWCC of the soil can be estimated directly from the grain-size distribution of the soil, particularly for a sandy soil.

Fig. 17. Air-entry value and residual matric suction for the drying soil-water characteristic curves versus grain-size parameter D_{10}.

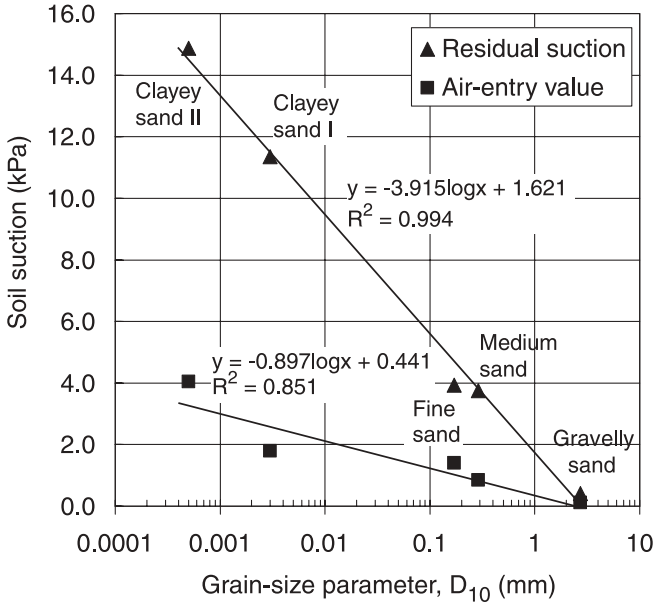

Fig. 18. Slope of drying soil-water characteristic curves versus slope of grain-size distribution curve of the soils.

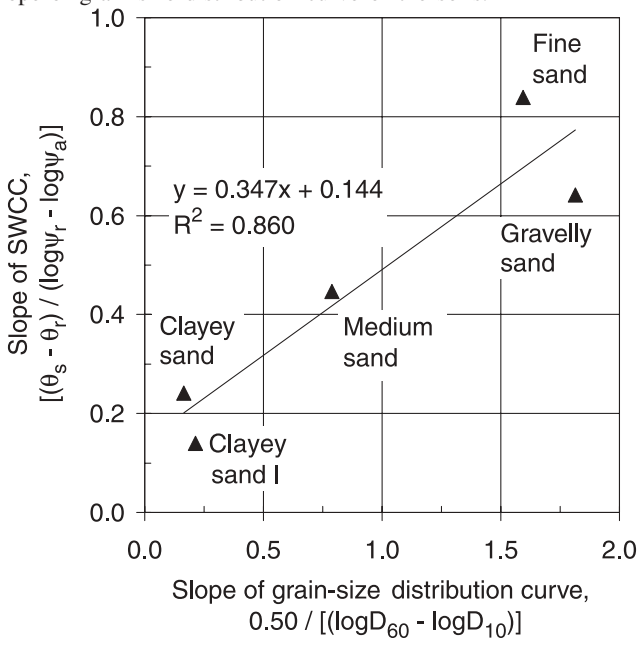

The effect of the porosity of the soil on the SWCC was demonstrated by conducting an additional Tempe pressure cell test on clayey sand II at a higher dry density (ρ_d = 1.70 Mg/m^3), and the results are shown in Fig. 20. Clayey sand II with a small porosity (dry density of 1.70 Mg/m^3) has an AEV of 11.0 kPa, which is higher than that corresponding to a large porosity (dry density of 1.47 Mg/m^3, see Table 1), where the AEV is 4.05 kPa (Table 2). This indicates that a soil with a smaller porosity has a higher AEV because of the smaller pore sizes in the soil. On the other hand, at a matric suction larger than the AEV, the SWCC with a smaller porosity is always above the SWCC corresponding to the soil with a larger porosity. This suggests that the volumetric water content in the denser soil (smaller porosity) can be higher than that in the less dense soil (large porosity) when the matric suction is higher than the AEV of the soils.

The effects of the grain-size distribution parameter (D_{10}) and porosity on the AEV of the SWCC as observed in this study were also consistent with those observed by Aubertin et al. (1998), who presented AEVs for some soils with different D_{10} values and void ratios (porosity). The results of Aubertin et al. showed that a large void ratio (or porosity) gave a small AEV for the same soil, and a large D_{10} gave a small AEV at a comparable void ratio.

3.4. Analysis of the wetting soil-water characteristic curves

The wetting SWCCs of the soils differ significantly from each other (Fig. 13), similar to the difference among the drying SWCCs (Fig. 12). The variations in the soil parameters for the wetting SWCCs are similar to those in the corresponding parameters for the drying SWCCs (i.e., Fredlund and Xing 1994 parameters as shown in Table 2). The fitting parameters a, m, and n (Table 2) control the shape of the wetting SWCC. The water-entry value of the wetting SWCC is also closely related to the grain-size parameter of the soil, D_{10} (Fig. 21). The water-entry value corresponds to the matric suction at which the water content of the soil starts to increase significantly during the wetting process. Therefore, the smallest pores in the soils as indicated by D_{10} to some extent must be first filled with water. A soil with a small D_{10} has a large water-entry value, i.e., the finer the soil particle, the higher the water-entry value of the soil, and the easier it is for the water to fill the pores of the soil.

3.5. Hysteresis of the soil-water characteristic curves

The results show that there is considerable hysteresis between the drying SWCC and the wetting SWCC for each soil (Figs. 7–11). The magnitude of the hysteresis of the five soils ranges from 0.2 logarithm cycles of suction for the fine sand to 1.1 logarithm cycles of suction for the clayey sand I near the inflection points on the curves. Hysteresis in the SWCCs indicates that the volumetric water content in the soil is not unique at a specific matric suction value but is related to the wetting and drying history of the soil. There does not appear to be much information with respect to the quantification of hysteresis between the drying and wetting SWCCs with soil properties. Therefore, the authors propose that the hysteresis between the drying and wetting SWCCs be quantified by total hysteresis, which is the area between the drying and wetting SWCCs as computed on a logarithm scale (Fig. 22). The larger the area, the higher the hysteresis. Total hysteresis represents the magnitude corresponding to the extreme situation of hysteresis. The plots of the total hysteresis versus D_{10} for the five soils in the study (Fig. 23) and the total hysteresis versus the tangent of the slope of the grain-size distribution curve (Fig. 24) show that the total hysteresis of soil appears to decrease with an increase in D_{10} and with an increase in the slope of the grain-size distribution curve. This suggests that a uniform, coarse-grained soil has a small total hysteresis.

Fig. 19. Soil-water characteristic curve estimated from the grain-size distribution for fine sand.

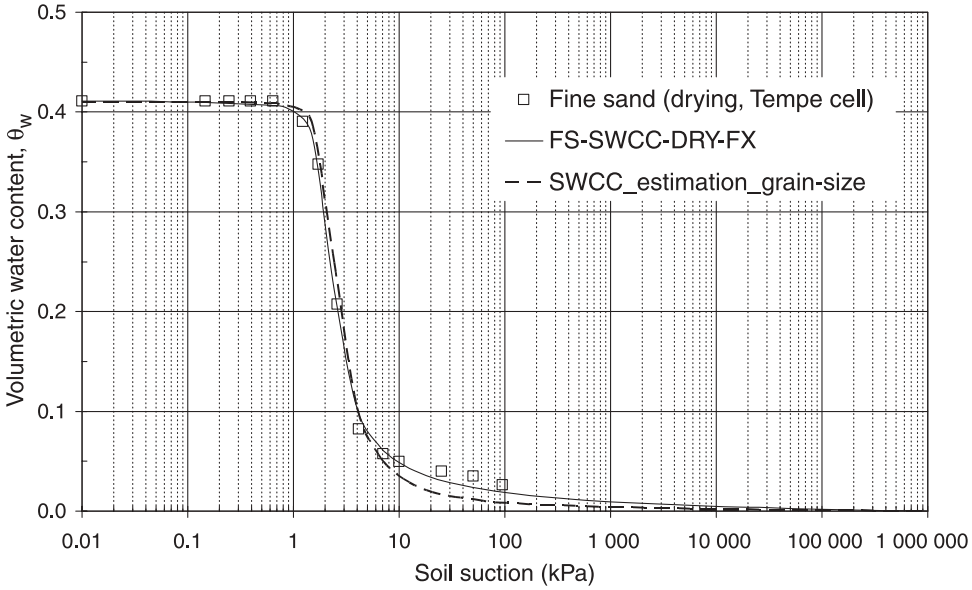

Fig. 20. Drying soil-water characteristic curves for clayey sand II under different dry densities.

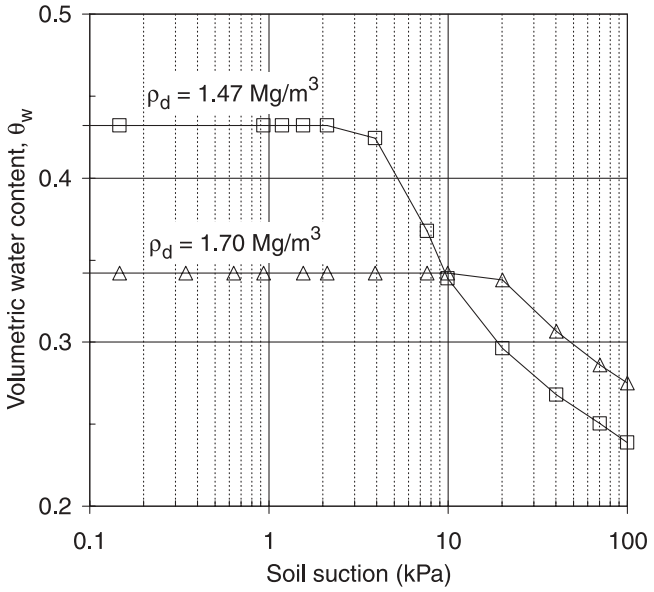

Fig. 21. Water-entry value versus grain-size parameter D_{10} for the soils.

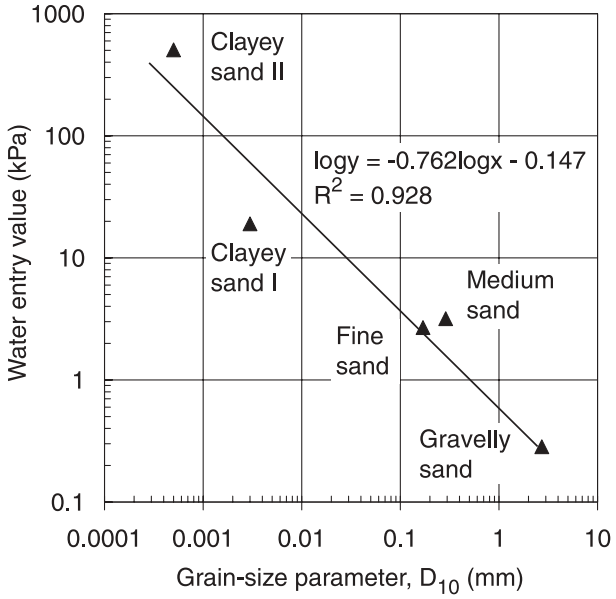

4. Summary and conclusions

Drying and wetting soil-water characteristic curves (SWCCs) were investigated for five soils, namely gravelly sand, medium sand, fine sand, clayey sand I, and clayey sand II, using Tempe pressure cell tests and capillary rise open tube tests. The SWCC test data for each soil were best-fitted using the Fredlund and Xing (1994) and van Genuchten (1980) equations. The SWCC was compared with that estimated from the grain-size distribution for fine sand. A drying SWCC was also performed for clayey sand II with a smaller porosity. The fitting parameters and hysteretic behaviour are discussed and correlated to the grain-size parameters. The concept of total hysteresis is proposed to quantify the hysteresis phenomenon.

The results show that the shapes of the SWCCs of the soils, as determined by the soil parameters, bear a consistent relationship to the grain-size distribution of the soils. A coarse-grained soil has a lower air-entry value, lower residual soil suction, and lower water-entry value than a fine-grained soil. A uniform, coarse-grained soil has a smaller total hysteresis than a less uniform, fine-grained soil. Hysteresis between the drying and wetting process is approximately 0.2–1.1 logarithm cycles of suction for the SWCCs of the soils investigated in this study. The SWCC of a uniform soil has a steeper slope than that of a less uniform soil. Soil with a large porosity has a lower air-entry value than soil with a small porosity.

Fig. 22. Total hysteresis of the soil-water characteristic curves for medium sand.

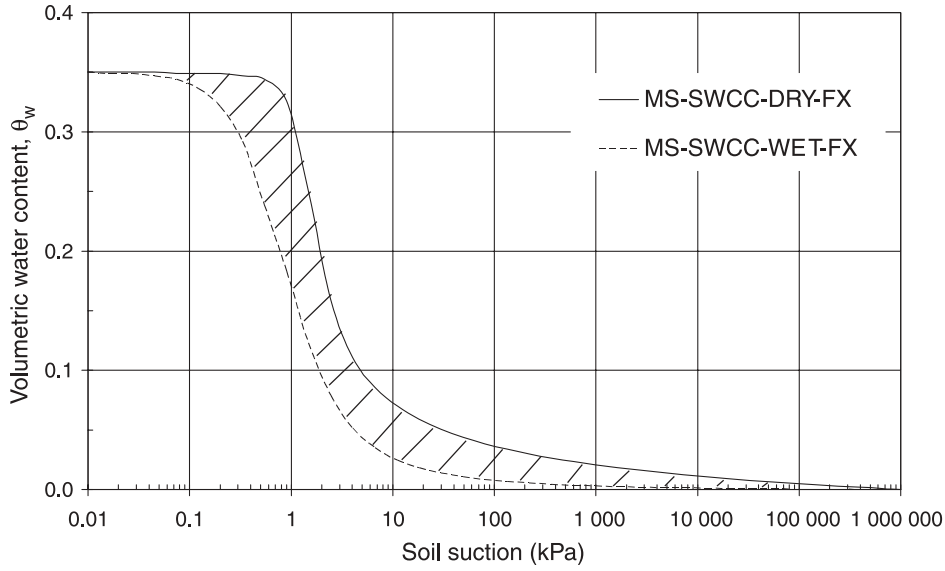

Fig. 23. Total hysteresis versus D_{10} for the soils.

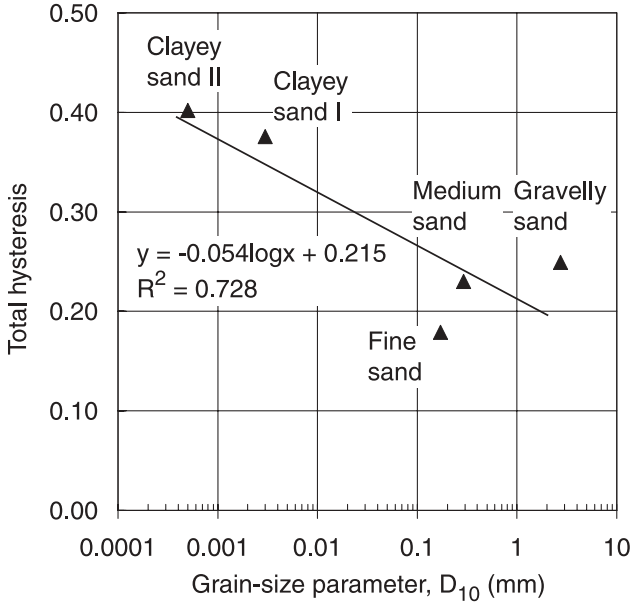

Fig. 24. Total hysteresis versus slope of grain-size distribution curves for the soils.

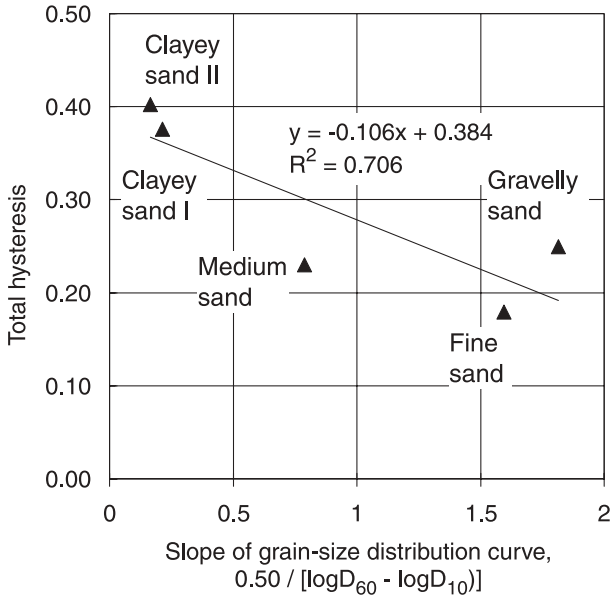

Acknowledgments

The authors gratefully acknowledge the financial assistance provided by the Nanyang Technological University, Singapore, for this research work under RG 7/99, Capillary barrier for slope stabilization, and ARC 12/96, Development of an instrument for field measurement of suction in unsaturated soil. The first author acknowledges the research scholarship received from the Nanyang Technological University, Singapore.

References

Arya, L.M., and Paris, J.F. 1981. A physicoempirical model to predict the soil moisture characteristic from particle-size distribution and bulk density data. Soil Science Society of America Journal, **45**: 1023–1030.

Assouline, S., Tessier, D., and Bruand, A. 1998. A conceptual model of the soil water retention curve. Water Resources Research, **34**(2): 223–231.

ASTM. 1997*a*. Standard test method for particle-size analysis of soils (D422-63). *In* 1997 Annual Book of ASTM Standards, Vol. 04.08. American Society for Testing and Materials (ASTM), Philadelphia, PA. pp. 10–16.

ASTM. 1997*b*. Standard test method for specific gravity of soils (D854-92). *In* 1997 Annual Book of ASTM Standards, Vol. 04.08. American Society for Testing and Materials (ASTM), Philadelphia, PA. pp. 88–91.

ASTM. 1997*c*. Standard test methods for amount of material in soils finer than the No. 200 (75-μm) sieve (D1140-92). *In* 1997 Annual Book of ASTM Standards, Vol. 04.08. American Soci-

ety for Testing and Materials (ASTM), Philadelphia, PA. pp. 92–94.

ASTM. 1997*d*. Standard test method for capillary-moisture relationships for coarse- and medium-textured soils by porous-plate apparatus (D2325-68). *In* 1997 Annual Book of ASTM Standards, Vol. 04.08. American Society for Testing and Materials (ASTM), Philadelphia, PA. pp. 195–201.

ASTM. 1997*e*. Standard classification of soils for engineering purposes (unified soil classification system) (D2487-93). *In* 1997 Annual Book of ASTM Standards, Vol. 04.08. American Society for Testing and Materials (ASTM), Philadelphia, PA. pp. 217–227.

ASTM. 1997*f*. Standard test method for liquid limit, plastic limit, and plasticity index of soils (D4318-95). *In* 1997 Annual Book of ASTM Standards, Vol. 04.08. American Society for Testing and Materials (ASTM), Philadelphia, PA. pp. 522–532.

Aubertin, M., Ricard, J.-F., and Chapuis, R.P. 1998. A predictive model for the water retention curve: application to tailings from hard-rock mines. Canadian Geotechnical Journal, **35**: 55–69.

Aubertin, M., Mbonimpa, M., Bussière, B., and Chapuis, R.P. 2003. A model to predict the water retention curve from basic geotechnical properties. Canadian Geotechnical Journal, **40**: 1104–1122.

Barbour, S.L. 1998. Nineteenth Canadian Geotechnical Colloquium: The soil-water characteristic curve: a historical perspective. Canadian Geotechnical Journal, **35**: 873–894.

Brooks, R.H., and Corey, A.T. 1964. Hydraulic properties of porous media. Colorado State University (Fort Collins), Hydrology Paper No. 3.

Brooks, R.H., and Corey, A.T. 1966. Properties of porous media affecting fluid flow. Journal of the Irrigation and Drainage Division, ASCE, **92**(IR2): 61–89.

Fredlund, D.G., and Rahardjo, H. 1993*a*. Soil mechanics for unsaturated soils. John Wiley & Sons Inc., New York.

Fredlund, D.G., and Rahardjo, H. 1993*b*. The role of unsaturated soil behaviour in geotechnical engineering practice. *In* Proceedings of the 11th Southeast Asian Geotechnical Conference, Singapore, March 1993. Southeast Asian Geotechnical Society, Pathumthani, Thailand. pp. 37–49.

Fredlund, D.G., and Xing, A. 1994. Equations for the soil-water characteristic curve. Canadian Geotechnical Journal, **31**: 521–532.

Fredlund, D.G., Xing, A., and Huang, S. 1994. Predicting the permeability function for unsaturated soils using the soil-water characteristic curve. Canadian Geotechnical Journal, **31**: 533–546.

Fredlund, M.D., Wilson, G.W., and Fredlund, D.G. 1997. Prediction of the soil-water characteristic curve from the grain-size distribution curve. *In* NSAT'97: Proceedings of the 3rd Symposium on Unsaturated Soil, Rio de Janeiro, Brazil, 20–22 April 1997. *Edited by* T.M.P. de Campos and E.A. Vargas. pp. 13–23.

Gupta, S.C., and Larson, W.E. 1979. Estimating soil water retention characteristics from particle size distribution, organic matter content, and bulk density. Water Resources Research, **15**(6): 1633–1635.

Haverkamp, R., and Parlange, J.Y. 1986. Predicting the water retention curve from particle size distribution: 1. Sandy soils without organic matter. Soil Science, **142**: 325–339.

Hogarth, W.L., Hopmans, J., Parlange, J.Y., and Haverkamp, R. 1988. Application of a simple soil-water hysteresis model. Journal of Hydrology, **98**: 21–29.

Holtz, R.D., and Kovacs, W.D. 1981. An introduction to geotechnical engineering. Prentice-Hall, Inc., Englewood Cliffs, NJ.

Jaynes, D.B. 1985. Comparison of soil-water hysteresis models. Journal of Hydrology, **75**: 287–299.

Klute, A. 1986. Water retention: laboratory methods. *In* Methods of soil analysis, part 1. *Edited by* A. Klute. Agronomy Monograph 9. 2nd ed. American Society of Agronomy and Soil Science Society of America, Madison, WI. pp. 635–662.

Lambe, T.W., and Whitman, R.V. 1979. Soil mechanics, SI version. John Wiley and Sons Inc., New York. pp. 245–246.

Leong, E.-C., and Rahardjo, H. 1997. Review of soil-water characteristic curve equations. Journal of Geotechnical and Geoenvironmental Engineering, ASCE, **123**(12): 1106–1117.

Mualem, Y. 1977. Extension of the similarity hypothesis used for modeling the soil water characteristics. Water Resources Research, **13**(4): 773–780.

Mualem, Y. 1984. Prediction of the soil boundary wetting curve. Journal of Soil Science, **137**(6): 379–390.

Mualem, Y. 1986. Hydraulic conductivity of unsaturated soils: prediction and formulas. *In* Methods of soil analysis, part 1. *Edited by* A. Klute. Agronomy Monograph 9. 2nd ed. American Society of Agronomy and Soil Science Society of America, Madison, WI. pp. 799–823.

Nimmo, J.R. 1992. Semi-empirical model of soil water hysteresis. Soil Science Society of America Journal, **56**: 1723–1730.

Parlange, J.Y. 1976. Capillary hysteresis and the relationship between drying and wetting curves. Water Resources Research, **12**(4): 224–228.

Pham, Q.H., Fredlund, D.G., and Barbour, S.L. 2003. A practical hysteresis model for the soil-water characteristic curve for soils with negligible volume change. Géotechnique, **53**(2): 293–298.

Rossi, C., and Nimmo, J.R. 1994. Modeling of soil water retention from saturation to oven dryness. Water Resources Research, **30**(3): 701–708.

Soilmoisture Equipment Corporation. 1985. Equipment specifications. Soilmoisture Equipment Corporation, Santa Barbara, CA.

Soilmoisture Equipment Corporation. 1999. Soilmoisture product catalog. Soilmoisture Equipment Corporation, Santa Barbara, CA.

SoilVision Systems Ltd. 1999. SoilVision: a knowledge-based database system for unsaturated–saturated soil properties (computer program), version 2.0. SoilVision Systems Ltd., Saskatoon, Sask.

Stormont, J.C., and Anderson, C.E. 1999. Capillary barrier effect from underlying coarse soil layer. Journal of Geotechnical and Geoenvironmental Engineering, ASCE, **125**(8): 641–648.

Topp, G.C., Galganov, Y.T., Ball, B.C., and Carter, M.R. 1993. Soil water desorption curves. *In* Soil sampling and methods of analysis. *Edited by* M.R Carter. Canadian Society of Soil Science, Lewis Publishers, Ann Arbor, MI. pp. 569–579.

Vanapalli, S.K., Fredlund, D.G., Pufahl, D.E., and Clifton, A.W. 1996. Model for the prediction of shear strength with respect to soil suction. Canadian Geotechnical Journal, **33**: 379–392.

Vanapalli, S.K., Sillers, W.S., and Fredlund, M.D. 1998. The meaning and relevance of residual state to unsaturated soils. *In* Proceedings of the 51st Canadian Geotechnical Conference, Edmonton, Alta., 4–7 October 1998. Canadian Geotechnical Society, Alliston, Ont.

van Genuchten, M.T. 1980. A closed-form equation for predicting the hydraulic conductivity of unsaturated soils. Soil Science Society of America Journal, **44**: 892–898.